Langmuir

Article

pubs.acs.org/Langmuir

A Phase-Field Approach for Wetting Phenomena of Multiphase Droplets on Solid Surfaces

Marouen Ben Said,*[,†] Michael Selzer,[†,‡] Britta Nestler,[†,‡] Daniel Braun,[§] Christian Greiner,[§] and Harald Garcke[∥]

[†]Institute of Applied Materials, Karlsruhe Institute of Technology, 76131 Karlsruhe, Germany

[‡]Institute of Materials and Processes, University of Applied Sciences, 76133 Karlsruhe, Germany

[§]Institute of Applied Materials, Karlsruhe Institute of Technology, 76344 Eggenstein-Leopoldshafen, Germany

[∥]Faculty of Mathematics, University of Regensburg, 93053 Regensburg, Germany

ABSTRACT: We study the equilibrium wetting behavior of immiscible multiphase systems on a flat, solid substrate. We present numerical computations which are based on a vector-valued multiphase-field model of Allen−Cahn type, with a new boundary condition, based on appropriately designed surface energy contributions in order to ensure the right contact angles at multiphase junctions. Experimental investigations are carried out to validate the method and to support the numerical results.

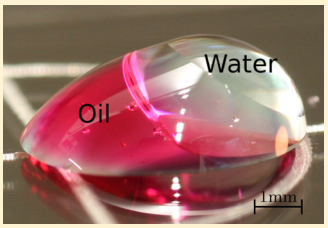

1. INTRODUCTION

The wetting behavior of liquids on solid surfaces has long been of interest to academic and industrial communities. More than 200 years ago, Young[1] presented a correlation between the equilibrium contact angle of a droplet surrounded by an immiscible fluid on a flat, chemically homogeneous, solid surface and the interfacial tensions in the liquid/solid/gas system. Among theoretical works[2−4] and experimental investigations,[5−10] numerical simulations have been established in the last 2 decades as powerful methods for the description and analysis of wetting phenomena.

It is well-known that the equilibrium shape of a droplet in contact with a solid surface is the one that minimizes its total interfacial energy at a fixed volume. Such a phenomenon can be seen as a free boundary problem, where the interface between two immiscible fluids (e.g., fluid droplet and surrounding air) is free and can change its shape in order to minimize its surface energy. In the last years, diffuse interface methods have become very popular to model such kinds of problems. Those consider the interface between two immiscible fluids to have a nonzero thickness endowed with physical properties, such as surface tension. Phase-field models are particular diffuse interface models, and their concept can be traced back to van der Waals.[11] For an overview on phase-field models and their applications, we refer to a number of selected review articles.[12,13]

In the context of wetting phenomena, Cahn[14] was the first to present a phase-field model with a wetting condition for a liquid in contact with a container wall. He extended the free energy formulation in the Cahn−Hilliard model[15] by a surface energy term, describing the interaction between the liquid and the solid wall. A discussion of Cahn's model and an asymptotic analysis can be found in refs 16 and 17, respectively. In order to ensure the right contact angles at the solid/liquid boundary, several so-called surface energy and geometric formulations were discussed in the literature,[18−25] to name a few. To ensure the volume conservation and the time-dependent relaxation dynamics of the liquid phase, the authors used a Cahn−Hilliard model. However, the proposed wetting conditions in the cited phase-field works are related to liquid/gas/solid systems, where the liquid phase consists of only one droplet and the equilibrium contact angle, θ_e, given by Young's law, is explicitly incorporated in the various formulations of the boundary condition. But what will happen if two or more droplets in contact with each other are placed on a solid surface? Which equilibrium shapes and contact angles will appear? To the best of our knowledge, so far there has been no phase-field approach capable of answering these questions.

The aim of this work is to present a new phase-field model with an integrated, physically motivated boundary condition to describe wetting processes of multiphase droplet ensembles in contact with flat and chemically homogeneous substrates. Instead of prescribing equilibrium angles, the boundary condition is consistently formulated in terms of the respective surface energies within an extended free energy functional and is derived by variational principles. Recent investigations[26−28] in various fields of application, where wetting is the crucial process, show the importance of understanding wetting behavior of immiscible multiliquid systems.

We emphasize that we are only interested in the equilibrium shapes and the equilibrium contact angles of the considered wetting systems. Therefore, we use an Allen−Cahn model with preserved volume fractions,[29,30] instead of a Cahn−Hilliard model. Due to the fact that both models are minimizing the

Received: January 27, 2014
Revised: March 27, 2014
Published: March 27, 2014

   dx.doi.org/10.1021/la500312q | *Langmuir* 2014, 30, 4033−4039

total free energy of the system, even though along different kinetic paths, they will lead to the same equilibrium solutions. However, the Allen–Cahn equations are easier to handle numerically, and therefore, the simulations will take fewer numerical time steps to reach the equilibrium state. Furthermore, we present an accurate boundary condition, ensuring the right contact angles at triple as well as multijunction points. Following the approaches given in refs 14 and 19, we write the total free energy $\mathcal{F} = \int_\Omega f \, d\Omega + \int_{\partial_s\Omega} f_w \, ds$, where f_w is a specific wall free energy, which only depends on the phase-field values at the solid wall ($\partial_s\Omega$), the physical properties of the phases, and the liquid/solid surface tensions. For multidroplet systems, the different equilibrium contact angles at multijunctions need not to be given explicitly in the boundary condition formulation. However, we show that the well-designed wall free energy contribution ensures the right contact angles at those critical points. The appropriateness of our model is supported by theoretical and experimental investigations.

The structure of the paper is as follows: in section 2, we introduce the modified phase-field model and derive an accurate boundary condition to simulate the wetting behavior of single droplet as well as multidroplet systems in contact with a flat, solid surface. The numerical discretisation scheme is described in section 3. In section 4, we first show that the new model recovers analytical results for single droplet systems well. Next, we will discuss numerical results for selected model systems consisting of immiscible droplet ensembles on a flat, solid surface surrounded by a gas phase. Finally, we compare and discuss numerical and experimental investigations of wetting structures observed for the real system consisting of a purified water droplet in contact with a poly-α-olefin oil droplet, where both fluids are placed on a flat, glass plate. A summary and conclusion is the subject of the last section.

2. PHASE-FIELD MODEL FOR MULTIPHASE SYSTEMS

In order to model wetting of immiscible multidroplet configurations on solid surfaces, we consider a general system consisting of N phases that can differ in their physical states. Each of the $N-1$ phases refers to a liquid droplet and the Nth phase represents the surrounding gas phase. We introduce a vector-valued continuous order parameter $\phi(\mathbf{x},t) = (\phi_1(\mathbf{x},t), ..., \phi_N(\mathbf{x},t))$, where each component $\phi_\alpha(\mathbf{x},t)$, $\alpha \in \{1, ..., N\}$, describes the state of the phase α in time and space. Since the volume of the droplets should be conserved, as we assume no evaporation, and no condensation and no chemical reaction take place, we will use a volume-preserved, diffuse interface formulation of a phase-field model for multiple order parameters, based on a Ginzburg–Landau energy density functional. A detailed description of the model can be found in refs 29 and 30. We write the energy density functional in the following form

$$\mathcal{F}(\phi) = \int_\Omega \left(\varepsilon a(\phi, \nabla\phi) + \frac{1}{\varepsilon} w(\phi) + g(\phi) \right) d\Omega \tag{1}$$

where Ω is the spatial domain and ε is a small positive parameter, related to the thickness of the diffuse interface, in which each order parameter $\phi_\alpha(\mathbf{x},t)$ varies continuously between two different physical states, $\phi_\alpha(\mathbf{x},t) = 0$ (in gas) and $\phi_\alpha(\mathbf{x},t) = 1$ (in liquid). Additionally, we postulate the constraint

$$\sum_{\alpha=1}^{N} \phi_\alpha(\mathbf{x}, t) = 1 \tag{2}$$

The gradient energy density, $a(\phi,\nabla\phi)$, can be formulated in terms of a generalized gradient vector $\mathbf{q}_{\alpha\beta} = \phi_\alpha\nabla\phi_\beta - \phi_\beta\nabla\phi_\alpha$ by

$$a(\phi, \nabla\phi) = \sum_{\alpha<\beta} \gamma_{\alpha\beta} |\phi_\alpha\nabla\phi_\beta - \phi_\beta\nabla\phi_\alpha|^2 \tag{3}$$

where $\gamma_{\alpha\beta}$ is the surface energy density of the α/β boundary. The vector $\mathbf{q}_{\alpha\beta}$ is the normal to the α/β interface. For our applications, we choose a multiobstacle potential $w(\phi)$ of the form

$$w(\phi) = \frac{16}{\pi^2} \sum_{\alpha<\beta} \gamma_{\alpha\beta}\phi_\alpha\phi_\beta + \sum_{\alpha<\beta<\delta} \gamma_{\alpha\beta\delta}\phi_\alpha\phi_\beta\phi_\delta \tag{4}$$

with a higher order term $\phi_\alpha\phi_\beta\phi_\delta$ that can be calibrated by the constant $\gamma_{\alpha\beta\delta}$ to suppress artificial third phase contributions along binary phase boundaries. The last term in the energy density functional is the bulk energy density $g(\phi)$, that ensures the volume preservation of each droplet. We use the expression

$$g(\phi) = \sum_{\alpha=1}^{N} \chi_\alpha h(\phi_\alpha) \tag{5}$$

with appropriate weights $\chi_\alpha = \chi_\alpha(t)$, which is discussed in ref 29. The function $h(\phi_\alpha)$ interpolates the phase-field values along the interfaces from zero to one. For the simulations we choose

$$h(\phi_\alpha) = \phi_\alpha^3(6\phi_\alpha^2 - 15\phi_\alpha + 10) \tag{6}$$

such that the first derivatives vanish in the bulk.

In order to model the interaction between the liquid droplets and the solid surface in a physically consistent manner, we extend the free energy formulation in eq 1 by an adequately designed solid–fluid interfacial energy density, f_w, which only depends on the fluid composition at the solid substrate. This way, the new free energy formulation reads

$$\mathcal{F}(\phi) = \int_\Omega \left(\varepsilon a(\phi, \nabla\phi) + \frac{1}{\varepsilon} w(\phi) + g(\phi) \right) d\Omega + \int_{\partial_s\Omega} f_w(\phi) \, dS \tag{7}$$

where

$$f_w(\phi) = \sum_{\alpha=1}^{N} \gamma_{\alpha s} h(\phi_\alpha) + m \sum_{\alpha<\beta<\delta}^{N} \phi_\alpha\phi_\beta\phi_\delta \tag{8}$$

The α/solid surface tensions are denoted by $\gamma_{\alpha s}$ for each phase $\alpha \in \{1, ..., N\}$. The higher order term $m\sum_{\alpha<\beta<\delta}^{N}\phi_\alpha\phi_\beta\phi_\delta$ in the wall energy formulation suppresses the occurrence of a nonphysical third phase in the interface between two liquid phases.[31] For the simulations we choose $m = 3$.

The surface integral in the above equation represents the solid–liquid and solid–gas interactions. At equilibrium, the total free energy $\mathcal{F}$ is at its minimum. The interface structure is obtained by minimizing the free energy functional eq 7 using methods of variational calculus. We use a steepest descent method which results in the following system of partial differential equations, for all phases $\alpha \in \{1, ..., N\}$

dx.doi.org/10.1021/la500312q | Langmuir 2014, 30, 4033–4039

$$\underbrace{\varepsilon(\nabla\cdot a_{,\nabla\phi_\alpha}(\phi,\nabla\phi) - a_{,\phi_\alpha}(\phi,\nabla\phi)) - \frac{1}{\varepsilon}w_{,\phi_\alpha}(\phi) - g_{,\phi_\alpha}(\phi)}_{:=\mathrm{rhs}_1} - \lambda_1 = \tau\varepsilon\partial_t\phi_\alpha \quad \text{in } \Omega \tag{9}$$

with the natural boundary condition

$$\underbrace{-\varepsilon a_{,\nabla\phi_\alpha}(\phi,\nabla\phi)n - f_{w,\phi_\alpha}(\phi)}_{:=\mathrm{rhs}_2} - \lambda_2 = 0 \quad \text{on } \partial_s\Omega \tag{10}$$

In the simulations, we set the relaxation parameter $\tau = 1$. The notation $a_{,\nabla\phi_\alpha}$, $a_{,\phi_\alpha}$, $w_{,\phi_\alpha}$, $g_{,\phi_\alpha}$, and f_{w,ϕ_α} is used to indicate the partial derivatives $\partial/\partial_{\nabla\phi_\alpha}$ and $\partial/\partial_{\phi_\alpha}$ of the functions $a(\phi,\nabla\phi)$, $w(\phi)$, $g(\phi)$, and $f_w(\phi)$, respectively. The divergence of the vector field $a_{,\nabla\phi_\alpha}(\phi,\nabla\phi)$ is denoted by $\nabla\cdot()$ and the time derivative $\partial_{\phi_\alpha}(\mathbf{x},t)/\partial t$ is denoted by $\partial_{t\phi_\alpha}$. The normal to the wall, $\partial_s\Omega$, is denoted by n. λ_1 and λ_2 are Lagrange multipliers, according to the constraint in eq 2.

$$\lambda_1 = \frac{1}{N^*}\sum_{\alpha=1}^{N^*}\mathrm{rhs}_1, \qquad \lambda_2 = \frac{1}{N^*}\sum_{\alpha=1}^{N^*}\mathrm{rhs}_2 \tag{11}$$

Here, N^* is the number of present phases in a particular computational cell (i, j, k). We define a phase α as the active phase if $\nabla_{\phi_\alpha}(i, j, k) \neq 0$. The boundary condition eq 10 stipulates that the liquid layer is always at equilibrium at the solid substrate, and the dynamic contact angle θ_D remains the same as the one at equilibrium, θ_e, as described by Jacqmin.[19] However, to study the contact line dynamics, the presented boundary condition must be modified in order to include the contact angle hysteresis and to allow θ_D to deviate from θ_e. Such wetting conditions are used when the phase-field model is coupled to a fluid flow model, as shown in refs 19 and 32. Given the objectives of the present work, we do not consider the effect of the contact angle hysteresis.

Moreover, we emphatically point out that, in contrast to other surface energy or geometric wetting formulations, no contact angles are explicitly prescribed in the formulation of the boundary condition. The evolution (eq 9) and the wetting condition (eq 10) only contain the involved liquid/gas, liquid/liquid, liquid/solid, and gas/solid surface tensions, which interact with each other in order to ensure the right equilibrium contact angles at all critical points of a wetting system.

3. NUMERICAL METHODS

We use a finite difference method on an equidistant Cartesian mesh with an explicit Euler time marching scheme to solve the set of phase-field equations 9 and the natural boundary condition (eq 10) numerically. We denote the time iteration by n with $n = 0, ..., Nt$ and the space coordinates by (i, j, k) with $i = 0, ..., Nx$; $j = 0, ..., Ny$; and $k = 0, ..., Nz$. The phase-field variables are defined at the center of each cell. Since we are only interested in the equilibrium shape of the wetting system where $\partial_{t\phi_\alpha} = 0$, for all phases $\alpha \in \{1, ..., N\}$, and since we stipulate that the liquid layer at the solid surface is at equilibrium for any time step, we substitute $\partial_{t\phi_\alpha} = 0$ in the boundary condition eq 10 to get

$$\partial_t\phi_\alpha = 2\varepsilon\left(\sum_{\substack{\beta=1\\ \beta\neq\alpha}}^{N^*}\gamma_{\alpha\beta}\phi_\beta\mathbf{q}_{\alpha\beta}n - \frac{1}{N^*}\sum_{\substack{\delta,\beta=1\\ \beta\neq\delta}}^{N^*}\gamma_{\delta\beta}\phi_\beta\mathbf{q}_{\delta\beta}n\right) - \left(\gamma_{\alpha s}h_{,\phi_\alpha}(\phi_\alpha) + m\sum_{\substack{\beta,\delta\neq\alpha\\ \beta<\delta}}^{N^*}\phi_\beta\phi_\delta - \frac{1}{N^*}\sum_{\alpha=1}^{N^*}\left(\gamma_{\alpha s}h_{,\phi_\alpha}(\phi_\alpha) + m\sum_{\substack{\beta,\delta\neq\alpha\\ \beta<\delta}}^{N^*}\phi_\beta\phi_\delta\right)\right) \tag{12}$$

$$\lambda_2 = \frac{1}{N^*}\left(2\varepsilon\sum_{\substack{\delta,\beta=1\\ \beta\neq\delta}}^{N^*}\gamma_{\delta\beta}\phi_\beta\mathbf{q}_{\delta\beta}n\right) + \frac{1}{N^*}\sum_{\alpha=1}^{N^*}\left(\gamma_{\alpha s}h_{,\phi_\alpha}(\phi_\alpha) + m\sum_{\substack{\beta,\delta\neq\alpha\\ \beta<\delta}}^{N^*}\phi_\beta\phi_\delta\right) \tag{13}$$

For a better readability, we use the notation $\phi_\alpha((i, j, k),t_n) := \phi^n_{\alpha,ijk}$, and without loss of generality, we set the solid boundary $\partial_s\Omega := \{(i, j, k) \in \Omega | j = 0\}$ with the normal vector $n = (0,1,0)^T$. Hence, eq 12 can be discretized as

$$\phi^{n+1}_{\alpha,i0k} = \phi^n_{\alpha,i0k} + 2\varepsilon\Delta t\left(\sum_{\substack{\beta=1\\ \beta\neq\alpha}}^{N^*}\gamma_{\alpha\beta}\phi^n_{\beta,i0k}(q_{\alpha\beta})_j - \frac{1}{N^*}\sum_{\substack{\delta,\beta=1\\ \beta\neq\delta}}^{N^*}\gamma_{\delta\beta}\phi^n_{\beta,i0k}(q_{\delta\beta})_j\right) - \Delta t\left(\gamma_{\alpha s}h_{,\phi_\alpha}(\phi^n_{\alpha,i0k}) + m\sum_{\substack{\beta,\delta\neq\alpha\\ \beta<\delta}}^{N^*}\phi^n_{\beta,i0k}\phi^n_{\delta,i0k} - \frac{1}{N^*}\sum_{\alpha=1}^{N^*}\left(\gamma_{\alpha s}h_{,\phi_\alpha}(\phi^n_{\alpha,i0k}) + m\sum_{\substack{\beta,\delta\neq\alpha\\ \beta<\delta}}^{N^*}\phi^n_{\beta,i0k}\phi^n_{\delta,i0k}\right)\right) \tag{14}$$

Here, $(q_{\alpha\beta})_j$ denotes a suitable approximation of the y-component of $\mathbf{q}_{\alpha\beta}$ at the solid boundary. The y-component of $\mathbf{q}_{\alpha\beta}$ is given as

$$(q_{\alpha\beta})_j = \phi_{\alpha,i0k}\frac{\partial\phi_\beta}{\partial y} - \phi_{\beta,i0k}\frac{\partial\phi_\alpha}{\partial y} \tag{15}$$

dx.doi.org/10.1021/la500312q | Langmuir 2014, 30, 4033−4039

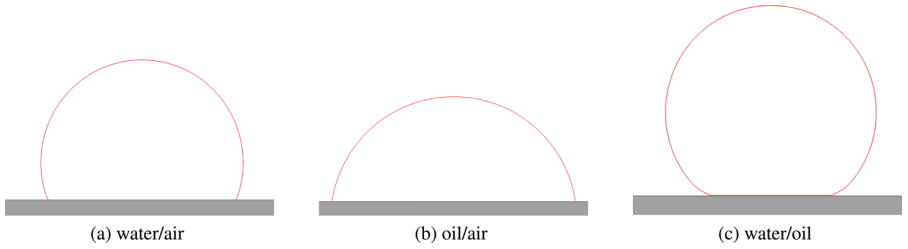

Figure 1. (a) Equilibrium shape of a water droplet surrounded by air, forming an equilibrium contact angle $\theta_{wa} = 112.4° \pm 1°$, (b) equilibrium shape of an oil droplet surrounded by air with an equilibrium contact angle $\theta_{oa} = 80.7° \pm 1°$, and (c) equilibrium shape of a water droplet surrounded by oil, establishing an equilibrium contact angle $\theta_{wo} = 147.2° \pm 1°$.

and depends on the unknown gradients of ϕ_α and ϕ_β at the solid boundary. In order to approximate this quantity, we first linearly extrapolate and temporarily store new phase-field values $\phi^n_{\alpha,i(-1)k}$, $i \in \{0, ..., Nx\}$, $k \in \{0, ..., Nz\}$, into ghost cells, located underneath the solid wall, according to

$$\phi^n_{\alpha,i(-1)k} = \frac{1}{2}\left(\frac{1}{2}\phi^n_{\alpha,i0k} - 4\phi^n_{\alpha,i1k} + \phi^n_{\alpha,i2k}\right) \tag{16}$$

and then we compute an approximation of the phase-field gradient normal to the boundary (without loss of generality in the y-direction) as

$$\frac{\partial \phi_\alpha}{\partial y} \approx \frac{\phi^n_{\alpha,i1k} - \phi^n_{\alpha,i(-1)k}}{2\Delta y} \tag{17}$$

In this manner, the approximations of the gradients are located at the center of the boundary cells $(i,0,k)$, where the boundary condition is executed.

4. RESULTS AND DISCUSSION

For systems consisting of a single droplet on a homogeneous, flat substrate surrounded by gas, we show that similar to the wetting conditions mentioned in refs 18−22, 25, 33, the new boundary condition also leads to Young's law. For such systems, the higher order term on the left-hand side of eq 8 vanishes and the wall energy contribution can be written as

$$f_w(\phi) = \gamma_{\alpha s} h(\phi_\alpha) + \gamma_{\beta s} h(\phi_\beta) = (\gamma_{\alpha s} - \gamma_{\beta s}) h(\phi) + \gamma_{\beta s} \tag{18}$$

Here, we use $h(\phi_\beta) = 1 - h(\phi_\alpha) =: 1 - h(\phi)$. The gradient energy density in eq 3 reduces to

$$a(\nabla\phi) = \gamma_{\alpha\beta} |\nabla\phi|^2 \tag{19}$$

and the natural boundary condition in eq 10 simplifies to

$$0 = 2\varepsilon\gamma_{\alpha\beta} \frac{\partial\phi}{\partial n} + (\gamma_{\alpha s} - \gamma_{\beta s}) \frac{\partial h(\phi)}{\partial \phi} \quad \text{on } \partial_s\Omega \tag{20}$$

An analysis of eq 20 across the liquid/gas interface along the solid boundary, as presented by Xu et al.,[33] shows that the boundary condition leads to Young's law, which describes the equilibrium contact angle for such wetting systems.

4.1. Experimental Investigations and Numerical Results. In this section, we compare numerical and experimental results of single droplet and multidroplet systems, as a validation of the presented multiphase-field model. Regarding the investigations on the purified water/poly-α-olefin (Klüber Lubricaton, Munich, Germany) system (simply called water/oil system), we first carry out experiments on the wetting behavior of each liquid on a silanized glass plate (called solid) separately, to determine the unknown water/solid, oil/solid, and air/solid surface tensions as essential input parameters for the simulations.

All experiments are carried out on microscope glass slides (VWR International, Radnor, PA). The glass slides are cleaned using piranha etch, a mixture of hydrogen peroxide and sulfuric acid (in the mixing ratio 5:1), to remove all the organic contamination and to provide a reproducible surface chemistry. The piranha cleaning is carried out for 12 h at room temperature. After cleaning, the surface is silanized using tridecafluoro-1,1,2,2-tetrahydrooctyl trichlorosilane (97%; abcr, Karlsruhe, Germany) and 2 μL of the silane is placed in a disposable aluminum bowl using disposable capillary pipettes. The bowl and the slides are put into a glass desiccator, which then is evacuated. After 12 h, the silanization process is finished and the glass slides are placed in an oven at 100 °C for 24 h. After this baking procedure, the contact angle measurements are carried out within 6 h. The measurements on silanized glass slides are performed with the sessile drop method. As equipment, an OCA-15 from Dataphysics (Filderstadt, Germany) is used.

4.1.1. Single Droplet Systems. At room temperature, we explore the equilibrium contact angles of water and oil surrounded by air and deposited on a solid substrate. Using the sessile drop method, we measure the equilibrium contact angles $\theta_{wa} = 112° \pm 3°$ for water and $\theta_{oa} = 81° \pm 3°$ for oil. The water/air and oil/air surface tensions are $\gamma_{wa} = 72.2 \times 10^{-3}$ N/m and $\gamma_{oa} = 25 \times 10^{-3}$ N/m, respectively. After exploring the contact angles of both systems experimentally, we determine the simulation parameters $(\gamma_{as} - \gamma_{ws})$ and $(\gamma_{as} - \gamma_{os})$ indirectly by using Young's law. Here, γ_{ws}, γ_{os}, and γ_{as} describe the water/solid, oil/solid, and air/solid surface tensions, respectively. The numerical results displayed in Figure 1a,b confirm the experimental issues. The contact angle measurements of the simulation results are performed by applying the fitting method suggested in ref 33. Furthermore, we measure the water/oil surface tension experimentally and obtain the value $\gamma_{wo} = (37 \times 10^{-3}) \pm (5 \times 10^{-3})$ N/m. The corresponding simulation of a water droplet surrounded by oil maintains an equilibrium contact angle $\theta_{wo} = 147.2° \pm 1°$ (see Figure 1c). This result will be taken into account in a further discussion below.

4.1.2. Multidroplet Systems.

Model Systems. To examine the accuracy of the model solutions for multiphase wetting systems, we study different model systems with two immiscible droplets α and β in contact with each other, surrounded by air and deposited on a flat, solid substrate, as illustrated in Figure 2. We perform simulations with different surface tension settings, as described in Table 1.

dx.doi.org/10.1021/la500312q | Langmuir 2014, 30, 4033−4039

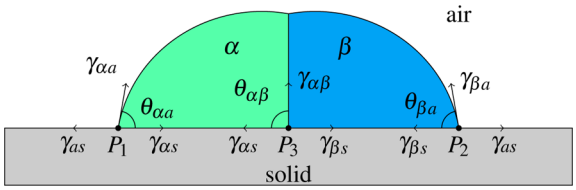

Figure 2. Scheme of two immiscible droplets surrounded by air and in contact with each other.

Table 1. Dimensionless Surface Tension Values for Three Different Wetting Systems

system	$\gamma_{\alpha s}$	$\gamma_{\beta s}$	γ_{as}	$\gamma_{\alpha s}$	$\gamma_{\beta a}$	$\gamma_{\alpha\beta}$
1	0.8	0.8	0.3	1	1	0.6
2	1	1	1	1	1	0.6
3	0.75	0.75	1	0.5	0.5	0.6

Applying Young's law at the triple points P_1, P_2, and P_3, we get the following system of equations, which describes the equilibrium contact angles $\theta_{\alpha a}$, $\theta_{\beta a}$, and $\theta_{\alpha\beta}$ as

$$\gamma_{\alpha a} \cos \theta_{\alpha a} = \gamma_{as} - \gamma_{\alpha s} \quad (21)$$

$$\gamma_{\beta a} \cos \theta_{\beta a} = \gamma_{as} - \gamma_{\beta s} \quad (22)$$

$$\gamma_{\alpha\beta} \cos \theta_{\alpha\beta} = \gamma_{\alpha s} - \gamma_{\beta s} \quad (23)$$

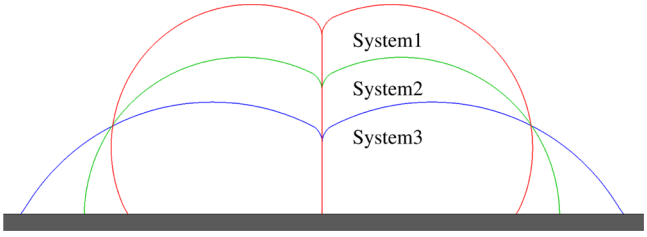

Figure 3. 2D equilibrium shapes of three different wetting systems consisting of two immiscible droplets.

Substitution of the surface tensions of Table 1 into the eqs 21−23 results in the theoretical contact angles listed in Table 2.

Table 2. Theoretical Contact Angles (in deg) Computed Using Young's Law and Measured Contact Angles (in deg) from the Simulation Data of the Model Systems

	theoretical			measured		
system	$\theta_{\alpha a}$	$\theta_{\beta a}$	$\theta_{\alpha a}$	$\theta^*_{\alpha a}$	$\theta^*_{\beta a}$	$\theta^*_{\alpha\beta}$
1	120	120	90	119.7 ± 1	119.7 ± 1	90 ± 1
2	90	90	90	90 ± 1	90 ± 1	90 ± 1
3	60	60	90	60.2 ± 1	60.2 ± 1	90 ± 1

For simplicity, we set $\gamma_{\alpha s} = \gamma_{\beta s}$ in the different model systems to ensure a theoretical contact angle $\theta_{\alpha\beta} = 90°$ at the triple point P_3. A 2D simulation with asymmetric liquid/solid surface tensions (i.e., $(\gamma_{\beta s} - \gamma_{\alpha s}) \neq 0$) shows a contact angle $\theta_{\alpha\beta} \neq 90°$ (see Figure 4). In real applications, the surface tensions are pairwise different in general, driving a partial or total engulfment of one droplet by the other. 2D simulations do not reflect this effect, such that 3D simulations are indispensable to get the proper equilibrium shapes, as shown in Figure 7c.

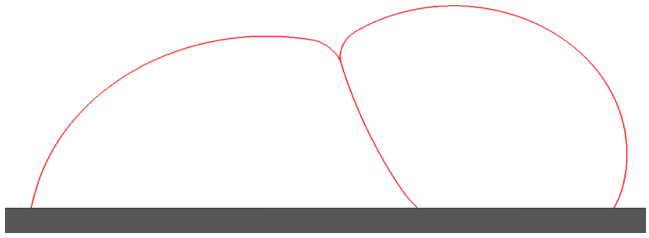

Figure 4. 2D equilibrium shape of two immiscible droplets with different liquid/solid surface tensions.

The simulations of the three and four immiscible droplet systems are performed by setting all the involved surface tensions equal to unity. As expected theoretically, the three contact angles, at the triple junction in the three droplets case, adjust at values 120° ± 1°, as shown in Figure 5. The triple

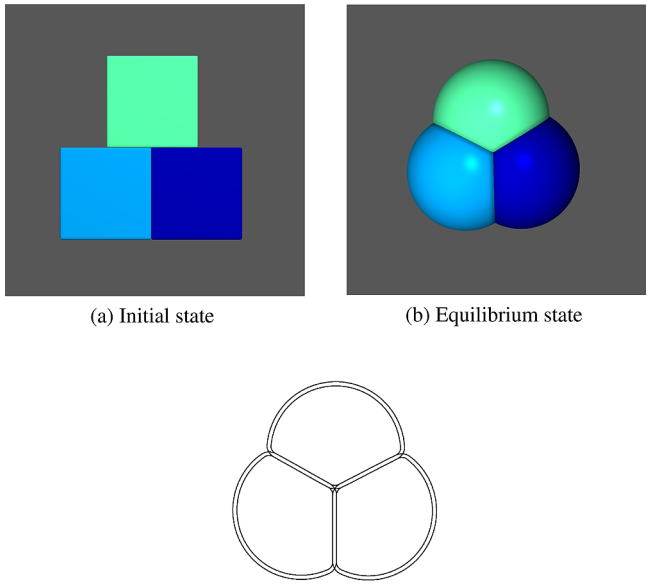

(a) Initial state (b) Equilibrium state

(c) 0.3 and 0.6 isolines at the solid boundary

Figure 5. Top view on the surface of simulated 3D droplets: (a) initial shape of three immiscible droplets surrounded by air and deposited on a flat, solid surface, (b) equilibrium shape at the end of the simulation, and (c) 0.3 and 0.6 isolines of the two-phase boundaries (outward to inward). The 0.3 isolines intersect at the triple junction where we measure three equilibrium contact angles close to 120° ± 1°.

junction is the intersection point of the three 0.3 isolines, where the three immiscible liquid phases coexist and exhibit the phase-field value $\phi_\alpha = 1/3$, $\alpha \in \{1, 2, 3\}$. The same result is obtained in grain growth computations with isotropic grain boundary characteristics,[31] a process which is also driven by surface tensions. Furthermore, the instability of the quadruple junction in the four droplets configuration is observed by Garcke et al.[31] in the context of moving grain boundaries in multigrain systems, where all grains exhibit the same surface tension, and is deeply discussed in the work of Srolovitz et al.[34] These authors, in particular, present a stability condition for the quadruple junction which is not fulfilled by the chosen surface tension setting. Therefore, the splitting of the quadruple junction into two triple junctions, that occurs in the simulation, is in accordance with the theoretical prediction (see Figure 6).

dx.doi.org/10.1021/la500312q | Langmuir 2014, 30, 4033−4039

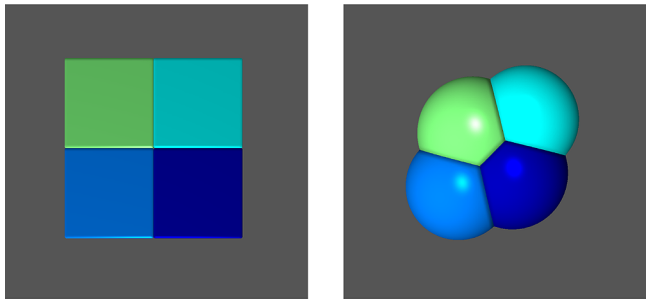

(a) Initial state (b) Equilibrium state

Figure 6. Top view of 3D phase-field simulations: (a) initial shape of four immiscible liquid phase regions surrounded by air and placed on a flat, solid surface, (b) instability of the quadruple point with a splitting into two triple junctions.

Water/Oil System. After the validation of the phase-field method combined with the appropriate wetting condition by means of the composed model systems, we will now consider the water/oil system mentioned at the beginning of this section. We depose two 5 μL immiscible droplets on the solid substrate simultaneously, and use colored oil to distinguish both liquids and to visualize the interface between them. Due to the hydrophilicity of the oil droplet, we experimentally observe how oil spreads along the substrate to finally border the water droplet by a thin layer. At equilibrium, we experimentally measure a contact angle of 81° ± 3° at the oil/air/solid contact line. This value is in agreement with the result presented in Figure 1b, where the equilibrium shape of an oil droplet surrounded by air is studied. Since no further experimental data of, for example, contact angle at the water/oil/solid contact line or the radius of the water/oil interface are available, a quantitative comparison between numerical and experimental results remains a challenge for future investigations. Nevertheless, a qualitative comparison of the equilibrium profiles in Figure 7a,b asserts a very good match of the experimental and

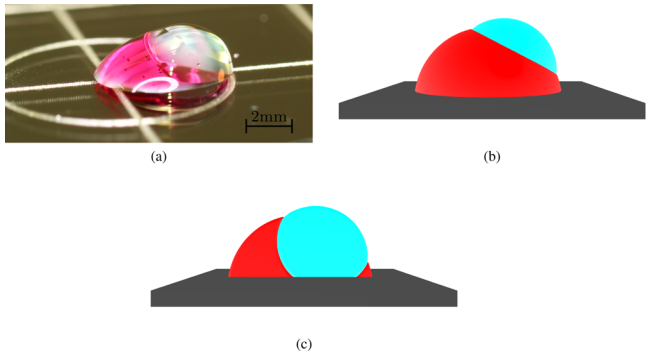

(a) (b) (c)

Figure 7. A qualitative comparison of the experimental and numerical equilibrium shapes. (a) Side view of the experimental photograph, (b) side view of the simulated droplet pair, and (c) plane along the middle slice through the droplets.

numerical equilibrium shape images. As illustrated in Figure 8, we also notice that the oil does not spread along the glass plate underneath the water droplet, neither in the experiment nor in the simulation. However, a linear combination of the eqs 21−23 shows that the contact angle at the water/oil/solid line depends on the two contact angles at the oil/air/solid and water/air/solid contact lines by

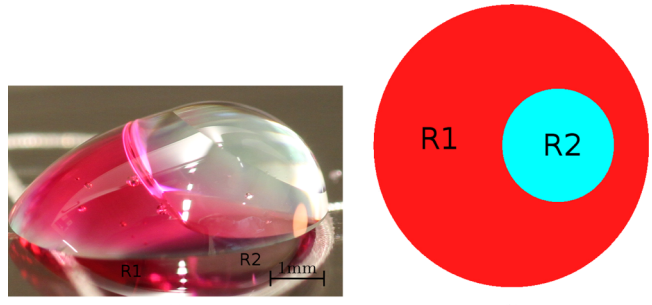

(a) (b)

Figure 8. The oil (magenta) engulfs but does not spread along the glass plate underneath the water droplet. (a) Reflections of oil and water on the glass plate are clearly visible in the regions R1 and R2, respectively. (b) Bottom view of the simulation along the solid surface.

$$\gamma_{\alpha a} \cos \theta_{\alpha a} - \gamma_{\beta a} \cos \theta_{\beta a} = \gamma_{\alpha\beta} \cos \theta_{\alpha\beta} \quad (24)$$

The subscripts α, β, a, and s denote water, oil, air, and solid, respectively. Since all the involved surface tensions, as well as the contact angles $\theta_{\alpha a}$ and $\theta_{\beta a}$, are given in section 4.1.1, using eq 24, we analytically compute $\theta_{\alpha\beta} \approx 147.6°$. By analyzing the phase boundaries along a cut in the middle of the simulation domain (see Figure 7c), we obtain a numerical angle of 146° ± 1°. The plausibility of this result can be based on the fact that the oil completely surrounds the water droplet within the plane of the solid substrate, as presented in Figure 7c. Furthermore, the resulting contact angle is in reasonable agreement with the computation in Figure 1c, related to the same wetting configuration (water surrounded by oil). Compared to the analytical result, the wetting angle at the water/oil/solid contact point in the simulation exhibits a discrepancy of less than 2%.

5. CONCLUSION

We present a multiphase-field model with a new wetting condition based on a surface energy formulation, which enables one to simulate the wetting phenomena of single droplet as well as immiscible multidroplet systems on a solid surface. We show that the formulation of the boundary condition is consistent with other formulations used in the literature for the wetting process of a single droplet. So, the key advantage of the generalized formulation is the ability to simulate the wetting behavior of immiscible multidroplet systems, and as shown, the presented numerical results agree with both the theoretical predictions as well as the experimental issues. The proposed model can be applied to predict the behavior of droplets on superhydrophobic surfaces, where the structured substrates are lubricant-impregnated.[28] To investigate the rolling off of the droplets (i.e., the contact line dynamics), the phase-field approach can be coupled to a two-phase fluid flow model[32,35] combined with extended boundary conditions in order to take the wall relaxation (i.e., contact angle hysteresis) into account. Further, we will also investigate the flow of two immiscible and incompressible fluids in a porous medium, including the wetting morphologies at the solid structure. The wetting properties of compound droplets on chemically heterogeneous surfaces will also be a topic of forthcoming computational investigations.

■ AUTHOR INFORMATION

Corresponding Author

*E-mail: marouen.bensaid@kit.edu

Notes

The authors declare no competing financial interest.

■ ACKNOWLEDGMENTS

We are grateful to A. Choudhury for many lively and fruitful discussions. We further thank the excellence center CCMSE of the state Baden Württemberg and the DFG project NE 822/20-1 for financial support.

■ REFERENCES

(1) Young, T. An essay on the cohesion of fluids. *Philos. Trans. R. Soc. London* **1805**, *95*, 65−87.
(2) Bormashenko, E. Young, Boruvka−Neumann, Wenzel and Cassie−Baxter equations as the transversality conditions for the variational problem of wetting. *Colloids Surf., A* **2009**, *345*, 163−165.
(3) Marmur, A. A guide to the equilibrium contact angles maze. In *Contact Angle Wettability and Adhesion*; Mittal, K. L., Ed.; Brill/VSP: Leiden, 2009; Vol. *6*, pp 3−18.
(4) Finn, R. *Equilibrium Capillary Surfaces*, Berger, M., Eckmann, B., Varadhan. S. R. S., Eds.; Springer-Verlag: New York, 1986.
(5) Butt, H.-J.; Graf, K.; Kappl, M. *Physics and Chemistry of Interfaces*; Wiley-VCH: Weinheim, Germany, 2003.
(6) Papadopoulos, P.; Deng, X.; Mammen, L.; Drotlef, D.-M.; Battagliarin, G.; Li, C.; Müllen, K.; Landfester, K.; del Campo, A.; Butt, H.-J. Wetting on the microscale: Shape of a liquid drop on a microstructured surface at different length scales. *Langmuir* **2012**, *28*, 8392−8398.
(7) Quéré, D. Wetting and roughness. *Annu. Rev. Mater. Res.* **2008**, *38*, 71−99.
(8) Extrand, C. Criteria for ultralyophobic surfaces. *Langmuir* **2004**, *20*, 5013−5018.
(9) Extrand, C.; Moon, S. I. Contact angles of liquid drops on super hydrophobic surfaces: Understanding the role of flattening of drops by gravity. *Langmuir* **2010**, *26*, 17090−17099.
(10) Extrand, C.; Moon, S. I. Which controls wetting? Contact line versus interfacial area: Simple experiments on capillary rise. *Langmuir* **2012**, *28*, 15629−15633.
(11) Van der Waals, J. Thermodynamische Theorie der Kapillarität unter voraussetzung stetiger Dichteänderung. *Z. Phys. Chem* **1894**, *13*, 657−725.
(12) Anderson, D.; McFadden, G.; Wheeler, A. Diffuse-interface methods in fluid mechanics. *Annu. Rev. Fluid Mech.* **1998**, *30*, 139−165.
(13) Boettinger, W.; Warren, J.; Beckermann, C.; Karma, A. Phase-field simulation of solidification 1. *Annu. Rev. Mater. Res.* **2002**, *32*, 163−194.
(14) Cahn, J. Critical point wetting. *J. Chem. Phys.* **1977**, *66*, 3667−6672.
(15) Cahn, J.; Hilliard, J. Free energy of a nonuniform system. I. Interfacial free energy. *J. Chem. Phys.* **1958**, *28*, 258−276.
(16) de Gennes, P. G. Wetting: Statics and dynamics. *Rev. Mod. Phys.* **1985**, *57*, 827−863.
(17) Modica, L. The gradient theory of phase transitions and the minimal interface criterion. *Arch. Ration. Mech. Anal.* **1987**, *98*, 123−142.
(18) Ding, H.; Spelt, P. D. M. Wetting condition in diffuse interface simulations of contact line motion. *Phys. Rev. E* **2007**, *75*, 046708.
(19) Jacqmin, D. Calculation of two-phase Navier−Stokes flows using phase-field modeling. *J. Comp. Phys* **1999**, *155*, 96−127.
(20) Jacqmin, D. Contact-line dynamics of a diffuse fluid interface. *J. Fluid Mech.* **2000**, *402*, 57−88.
(21) Khatavkar, V.; Anderson, P.; Meijer, H. Capillary spreading of a droplet in the partially wetting regime using a diffuse-interface model. *J. Fluid Mech.* **2007**, *572*, 367−387.
(22) Lee, H.; Kim, J. Accurate contact angle boundary conditions for the Cahn−Hilliard equations. *Comput. Fluids* **2011**, *44*, 178−186.
(23) Papatzacos, P. Macroscopic two-phase flow in porous media assuming the diffuse-interface model at pore level. *Transp. Porous Media* **2002**, *49*, 139−174.
(24) Seppecher, P. Moving contact lines in the Cahn−Hilliard theory. *Int. J. Eng. Sci.* **1996**, *34*, 977−992.
(25) Villanueva, W.; Amberg, G. Some generic capillary-driven flows. *Int. J. Multiphase Flow* **2006**, *32*, 1072−1086.
(26) Bormashenko, E.; Pogreb, R.; Balter, R.; Gendelman, O.; Aurbach, D. Composite non-stick droplets and their actuation with electric field. *Appl. Phys. Lett.* **2012**, *100*, 151601−151604.
(27) Friberg, S. Selective emulsion inversion in an equilibrium Janus drop. 1. Unlimited space. *J. Colloid Interface Sci.* **2014**, *416*, 167−171.
(28) Smith, J. D.; Dhiman, R.; Anand, S.; Reza-Garduno, E.; Cohen, R. E.; McKinley, G. H.; Varanasi, K. K. Droplet mobility on lubricant-impregnated surfaces. *Soft Matter* **2013**, *9*, 1772−1780.
(29) Nestler, B.; Wendler, F.; Selzer, M.; Stinner, B.; Garcke, H. Phase-field model for multiphase systems with preserved volume fractions. *Phys. Rev. E* **2008**, *78*, 0116041−0116047.
(30) Garcke, H.; Nestler, B.; Stinner, B.; Wendler, F. Allen−Cahn systems with volume constraints. *Math. Models Methods Appl. Sci.* **2008**, *18*, 1347−1381.
(31) Garcke, H.; Nestler, B.; Stoth, B. A multiphase field concept: Numerical simulations of moving phase boundaries and multiple junctions. *SIAM J. Appl. Math.* **1999**, 295−315.
(32) Salgado, A. J. A diffuse interface fractional time-stepping technique for incompressible two-phase flows with moving contact lines. *ESAIM, Math. Model. Numer. Anal.* **2013**, *47*, 743−769.
(33) Xu, X.; Wang, X. Derivation of the Wenzel and Cassie equations from a phase field model for two phase flow on rough surface. *SIAM J. Appl. Math.* **2010**, *70*, 2929−2941.
(34) Srolovitz, D. J.; Holm, E. A.; Cahn, J. Modeling microstructural evolution in two-dimensional two-phase microstructures. *Mater. Sci. Forum* **1992**, *94*−*96*, 141−158.
(35) Abels, H.; Garcke, H.; Grün, G. Thermodynamically consistent, frame indifferent diffuse interface models for incompressible two-phase flows with different densities. *Math. Methods Appl. Sci.* **2012**, *22*, 1150013-1−1150013-40.